

III.A.26 Electrocatalytically Active High Surface Area Cathodes for Low Temperature SOFCs

Objectives

- Develop a fundamental understanding of heterogeneous electrocatalytic phenomena at the surface of ion conducting ceramics.
- Fabricate high surface area SOFC cathodes with controlled microstructure and porosity.
- Develop cathodes for low to intermediate temperature SOFCs.

Accomplishments

- Optimized high performance Ag-erbium-stabilized bismuth oxide (ESB) cathode with low area specific resistance (ASR).
- Demonstrated stability issues of Ag-ESB composite cathodes.
- Improved stability of Ag-ESB composite cathodes by addition of 10-15 vol% nano-scale yttria-stabilized zirconia (YSZ) powder.
- Synthesized nano-sized bismuth ruthenate ($\text{Bi}_2\text{Ru}_2\text{O}_7$), lead ruthenate ($\text{Pb}_2\text{Ru}_2\text{O}_7$) and praseodymium-doped yttrium ruthenate ($\text{Y}_{2-x}\text{Pr}_x\text{Ru}_2\text{O}_7$) powders via co-precipitation method and a novel wet chemical route.
- Developed higher conductivity $\text{Y}_{2-x}\text{Pr}_x\text{Ru}_2\text{O}_7$ resulting in lower ASR cathodes.
- Determined the effects of microstructure and thickness on ASR of $\text{Bi}_2\text{Ru}_2\text{O}_7$ -ESB composite cathodes.
- Developed high performance $\text{Bi}_2\text{Ru}_2\text{O}_7$ -ESB composite cathodes with an ASR of $0.03 \Omega\text{cm}^2$ at 700°C .

Eric D. Wachsman

Department of Materials Science and Engineering
University of Florida
Gainesville, FL 32611-6400
Phone: (352) 846-2991; Fax: (352) 846-0326
E-mail: ewach@mse.ufl.edu

DOE Project Manager: Lane Wilson

Phone: (304) 285-1370
E-mail: Lane.Wilson@netl.doe.gov

Introduction

For extensive deployment of SOFCs into industrial and consumer markets to become a reality, further performance optimization is necessary. Currently cathode overpotential is the most significant drag on total SOFC *electrochemical* performance. A significant increase in cathode performance would enable higher power densities at lower temperature, which would mean lower cost and therefore greater commercial viability. Towards that end, we are in the process of developing high performance cathodes for use in conventional and intermediate to low temperature SOFCs.

Approach

We have focused our cathode research on pyrochlore ruthenates because of two reasons. First, the pyrochlore structure has proven to have very tunable conductivity. Depending on the characteristics of the A- and B-site cations, pyrochlores can be designed to be insulating, ionically conducting, semi-conducting or even metallic conducting ($\sim 10^3 \text{ S/cm}$). Second, ruthenium oxide is known to be catalytic active towards oxygen reduction so it can be expected that these ruthenates will have low activation polarization when used as SOFC cathodes.

To develop pyrochlore ruthenates for SOFC cathodes two approaches were used: (1) compositional optimization to maximize electrical conductivity and (2) microstructural optimization to minimize the ASR. The results of these efforts are described below.

Results

1. Compositional Development and Processing of Pyrochlore Ruthenates.

Lead ruthenate, $\text{Pb}_2\text{Ru}_2\text{O}_{6.5}$ (PRO), has been studied and reported in the literature as a potential high performance cathode material [1]. Our studies of PRO have been focused on making nano-sized powders for use in composite electrodes. Through novel processing we have been able to achieve our goals and were able to produce nano-sized lead ruthenate crystallites. This was discussed in greater detail in our previous report.

Yttrium ruthenate, $\text{Y}_2\text{Ru}_2\text{O}_7$ (YRO) has been evaluated as a candidate IT-SOFC cathode because of its stability in a wide range of temperature and its lack of reactivity in contact with yttria-stabilized zirconia and gadolinia-doped ceria [2]. We prepared, nanocrystalline powders of YRO by a co-precipitation method. Phase and morphology were studied by x-ray diffraction (XRD) and field emission scanning electron microscope (FE-SEM), showing a particle size of about 100 nm. The nanocrystalline particle size makes the powder amenable for the triple phase boundary tailoring in order to minimize ASR.

The electronic behavior of ruthenium pyrochlores is explained in terms of the Mott–Hubbard mechanism of electron localization, which shows high electrical (metallic) conductivity when their structure allows a Ru–O–Ru bond angle larger than 133° [3]. Moreover, since the Ru–O–Ru angle increases with increasing size of the A cation, Pr was chosen as an A-site dopant in order to increase the electrical conductivity of yttrium ruthenate.

X-ray diffraction studies confirmed that the doped powders were single pyrochlore phase, and SEM-EDS measurements confirmed the presence of the dopant in the pyrochlore structure. The electrical conductivity was measured at several temperatures by the d.c. 4-probe method, for a range of 5–25% dopant concentration, in a range of 473–1,073 K. Our results, Figure 1, show that doping with Pr significantly increases the conductivity of yttrium ruthenate.

Figure 1 shows a comparison of the total electrical conductivity of bismuth ruthenate, lead ruthenate, and Pr-doped yttrium ruthenate as a function of reciprocal temperature. In general, it shows that bismuth ruthenate and lead ruthenate are significantly more

conductive than the yttrium ruthenates. Moreover, bismuth ruthenate and lead ruthenate display metallic-type conductivity while the yttrium ruthenates are semiconducting.

Figure 1 also shows the effect of doping yttrium ruthenate with Pr. As the Pr content increases so does the overall conductivity. Our studies on the conductivity dependence of praseodymium-doped yttrium ruthenate on oxygen partial pressure (P_{O_2}) showed insensitivity to P_{O_2} changes. This suggests the observed increase in conductivity over undoped yttrium ruthenate is due mainly to the size effect of Pr increasing electronic the conductivity through the aforementioned Mott–Hubbard mechanism of electron localization. More tests will be conducted to confirm this inference. Nevertheless, Pr-doped yttrium ruthenate shows potential for use as a high performance SOFC cathode on YSZ.

2. Microstructural Optimization of Bismuth Ruthenate

Phase-pure $\text{Bi}_2\text{Ru}_2\text{O}_{7.0}$ (BRO) and $\text{Er}_{0.4}\text{Bi}_{1.6}\text{O}_3$ (ESB) were obtained by conventional solid-state synthesis. Leaching with HNO_3 was required to remove the Bi-rich sillenite phase from the BRO powders. Powders were then crushed and sieved. A portion of these powders were then vibratory milled to reduce particle size. Particle size distributions were narrowed using sedimentation. Powders containing large-size particles—those which have been sieved but not vibratory milled—are designated with a subscript “S”. Powders containing small-size particles—those which have been vibratory milled—are designated with a subscript “VM”.

Electrode ink slurries were prepared by combining a 50–50 wt% mixture of BRO and ESB powders with appropriate organic vehicles. Four different inks were prepared, using the different particle size combinations— BRO_S - ESB_S , BRO_S - ESB_{VM} , BRO_{VM} - ESB_S , and BRO_{VM} - ESB_{VM} . The inks were applied to both sides of dense ESB pellets, dried, and fired at 800°C for 2 h. The symmetrical cells were then electrochemically tested using impedance spectroscopy.

An Arrhenius plot of the electrode ASR for the four different microstructures is shown in Figure 2. Both composites containing coarse BRO particles have the highest ASRs while both composites containing fine BRO particles have the lowest ASRs. The composite composed of fine particles of both phases has the lowest ASR ($0.074\ \Omega\text{cm}^2$ at 650°C and $0.048\ \Omega\text{cm}^2$ at 700°C).

For comparison, the two lowest-ASR cathode systems prepared without sedimentation are also plotted in the figure (BRO_{VM} - ESB_{VM} and BRO_{VM} - ESB_S). These two systems exhibit the lowest ASR after sedimentation, but the order is reversed, and the values are significantly lower (50–85% reduction in ASR). The reduced particle size distribution translates into a larger number fraction

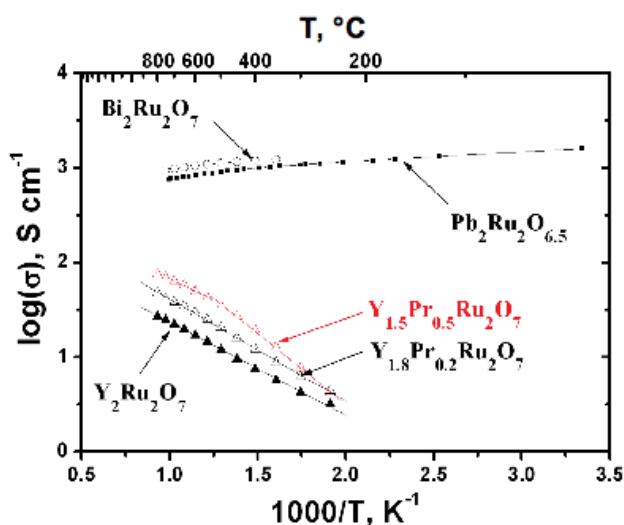


FIGURE 1. Comparison of Temperature-Dependent Conductivity of Ruthenate Pyrochlores

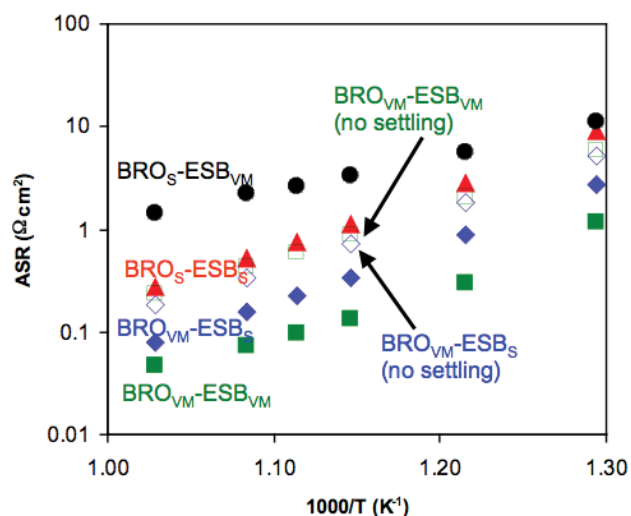


FIGURE 2. Arrhenius Plot of Nominally-Similar BRO-ESB Cathodes Containing Different Microstructures for Powders with Sedimentation (closed symbols) and without Sedimentation (open symbols)

of sub-micron sized particles in the vibratory milled phase. This in turn translates into longer three-phase boundary (TPB) lines between the oxidant (air), the ion-conducting phase (ESB) and the electron conducting phases (BRO). The fact that the $\text{BRO}_{\text{VM}}\text{-ESB}_{\text{VM}}$ system (where both phases are composed of vibratory-milled powder) exhibits the most dramatic reduction in ASR after sedimentation gives credence to this argument.

In order to improve the connectivity of the two phases in the composite and reduce lateral resistance, the thickness of the electrodes was increased. Additional layers were added after drying of the previous layers. For each microstructurally distinct electrode system, cells having one, two, and four coats of electrode material were tested. Additionally, for each of the four systems, a pure BRO_S current collector was added to a pellet coated twice with the electrode ink. Just before testing the samples, a multimeter was used to ensure the lateral resistance of each was at or below 1 Ω .

The results of these studies are shown in Figure 3. For the composite system shown (and for all other systems), ASR decreased with number of coatings. The addition of a pure BRO_S current collector to these cathode systems results in a more dramatic reduction in ASR than changes in thickness alone. A minimum ASR was achieved for the $\text{BRO}_{\text{VM}}\text{-ESB}_S$ system, with a value of 0.054 Ωcm^2 at 650°C and 0.034 Ωcm^2 at 700°C. Further improvement is expected with the $\text{BRO}_{\text{VM}}\text{-ESB}_{\text{VM}}$ system.

This particular system exhibits the lowest ASR produced to date by our research group, and is compared against a literature survey as well as some of our group's earlier results in Figure 4. Shown is a comparison between the ASR vs. 1/T profiles for

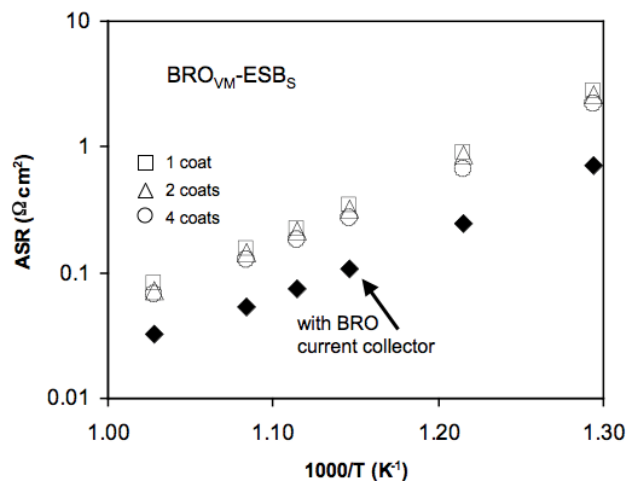


FIGURE 3. Arrhenius plot of ASR for the $\text{BRO}_{\text{VM}}\text{-ESB}_S$ system at various thicknesses with no current collector (open symbols). Also shown is the same system with two coats of the electrode ink and a pure BRO_S current collector (closed symbols).

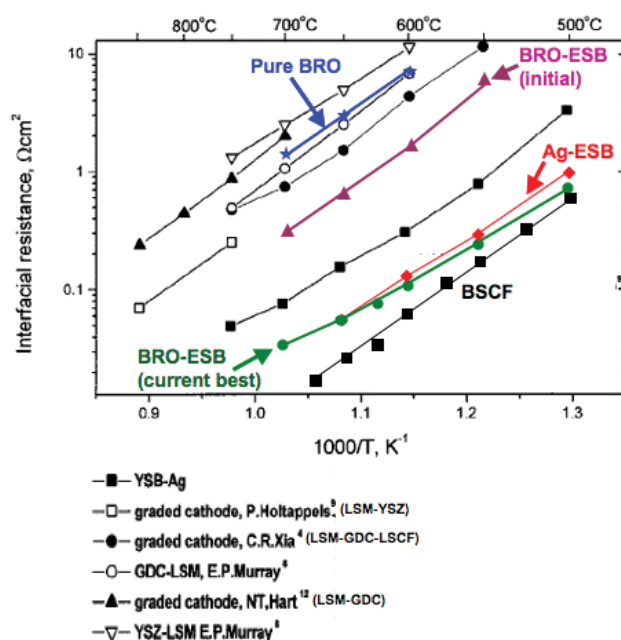


FIGURE 4. Arrhenius plot of ASR for the current optimized cathode system with some previous results. Also shown is the BSCF system, overlaid on a recent literature survey of composite cathode systems.

(i) an optimized Ag-ESB system, (ii) pure BRO (no ESB phase), (iii) a compositionally-optimized BRO-ESB system without any microstructural considerations (initial), the lowest ASR BRO-ESB system obtained to date (current best) and a composite literature survey from C. Xia, et. al [4], as well as the results from Z. Shao and S.M. Haile [5] for $\text{Ba}_{0.5}\text{Sr}_{0.5}\text{Co}_{0.8}\text{Fe}_{0.2}\text{O}_{3-\delta}$ (BSCF) cathodes which exhibit the lowest ASR reported to date in the literature.

The current microstructurally optimized BRO-ESB composite is approaching those values reported for barium strontium cobalt ferrite (BSCF). Additionally, the lower activation energy of BRO-ESB (~1.04 eV) compared to that of BSCF (~1.20 eV) should translate to better performance at lower temperatures. Initial long-term stability studies on the BRO-ESB cathode system under fuel cell operating conditions show it to be very stable, with a rise in cathode polarization of only a few percent over 500 h at 625°C. We have not been able to achieve similar stability with the BSCF system.

Conclusions and Future Directions

- Synthesized nano-sized $\text{Bi}_2\text{Ru}_2\text{O}_7$, $\text{Pb}_2\text{Ru}_2\text{O}_7$ and doped $\text{Y}_2\text{Ru}_2\text{O}_7$ powders via co-precipitation and a novel wet chemical route.
- Increased $\text{Y}_2\text{Ru}_2\text{O}_7$ conductivity by 20% by doping with 15 mol% Pr.
- Developed stable, low ASR $\text{Bi}_2\text{Ru}_2\text{O}_7$ -ESB composite cathodes.
- Optimized the microstructure of $\text{Bi}_2\text{Ru}_2\text{O}_7$ -ESB composite cathodes with an ASR of $0.03 \Omega\text{cm}^2$ at 700°C.

FY 2006 Publications/Presentations

1. "Novel Bismuth Ruthenate based Cathodes for IT-SOFCs; Part I: Doped Bismuth Ruthenates," A. Jaiswall and E.D. Wachsman, *Solid State Ionics*, submitted.
2. "Applicability of $\text{Bi}_2\text{Ru}_2\text{O}_7$ Pyrochlore Electrodes for ESB and BiMEVOX Electrolytes," V. Esposito, E. Traversa, and E.D. Wachsman, *Journal of the Electrochemical Society*, accepted.
3. "Synthesis and Characterization of $\text{Y}_{2-x}\text{Pr}_x\text{Ru}_2\text{O}_7$ and $\text{Y}_{2-x}\text{Pr}_x\text{Ru}_2\text{O}_7$ for the Cathode Application in Intermediate

Temperature Solid Oxide Fuel Cells," C. Abate, K. Duncan, V. Esposito, E. Traversa, and E. D. Wachsman, *Solid State Ionic Devices IV, ECS Transactions*, E.D. Wachsman, F.H. Garzon, E. Traversa, R. Mukundan, and V. Birss, Ed., **1-7**, 255-262 (2006).

4. " $\text{Bi}_2\text{Ru}_2\text{O}_7$ Pyrochlore Electrodes for Bi_2O_3 Based Electrolyte for IT-SOFC Applications," V. Esposito, B. H. Luong, E. Di Bartolomeo, E. D. Wachsman, and E. Traversa, *Solid State Ionic Devices IV, ECS Transactions*, E.D. Wachsman, F.H. Garzon, E. Traversa, R. Mukundan, and V. Birss, Ed., **1-7**, 263-278 (2006).

5. " $\text{Ag-Bi}_{1.6}\text{Er}_{0.4}\text{O}_3$ as a Potential Cathode Material for IT-SOFCs," M. Camaratta and E. D. Wachsman, *Solid State Ionic Devices IV, ECS Transactions*, E.D. Wachsman, F.H. Garzon, E. Traversa, R. Mukundan, and V. Birss, Ed., **1-7**, 279-292 (2006).

6. "Direct Current Bias Studies on $(\text{Bi}_2\text{O}_3)_{0.8}(\text{Er}_2\text{O}_3)_{0.2}$ Electrolyte and $\text{Ag}-(\text{Bi}_2\text{O}_3)_{0.8}(\text{Er}_2\text{O}_3)_{0.2}$ Cermet Electrode," A. Jaiswall and E.D. Wachsman, *Solid State Ionics*, **177** (7-8), 677-685 (2006).

7. " $\text{Pb}_2\text{Ru}_2\text{O}_{6.5}$ as a Low-Temperature Cathode for Bismuth Oxide Electrolytes," V. Esposito, E. Traversa, and E.D. Wachsman, *Journal of the Electrochemical Society*, **152** (12), A2300-2306 (2005).

References

1. J. Prakash, D. Tryk, and E. B. Yeager, *J. Electrochem. Soc.*, **146** (1999) 4145.
2. A. Bencan, M. Hrovat, J. Holc, and M. Kosec, *Materials Research Bulletin* **35**, (2000) 2415.
3. K. S. Lee, *J. Solid State Chem.* **131** (1997), 405.
4. C.R. Xia, Y. Zhang, M.L. Liu, *Applied Physics Letters*, **82** (2003) 901.
5. Z. Shao, S. M. Haile, *Nature*, **431** (2004) 170.